The geometric structure of Rb/Cu(111) investigated with X-ray standing waves: Rb coverage dependence

D. Heskett [a,*], P. Xu [a], L. Berman [b], C.-C. Kao [b], M.J. Bedzyk [c,d]

[a] Department of Physics, University of Rhode Island, Kingston, RI 02881, USA
[b] National Synchrotron Light Source, Brookhaven National Laboratory, Upton, NY 11973, USA
[c] Department of Materials Science and Engineering, Northwestern University, Evanston, IL 60208, USA
[d] Argonne National Laboratory, Materials Science Division, Argonne, IL 60439, USA

Abstract

We have carried out a back reflection X-ray standing wave (BRXSW) investigation of the geometric structure and degree of ordering of the system Rb/Cu(111) as a function of Rb coverage. We observe no change in the Rb–Cu(111) perpendicular spacing as a function of coverage from saturation coverage of $\theta = 1/4$ down to a coverage of $\theta = 1/16$. We find a high degree of ordering of the Rb atoms perpendicular to the surface at all coverages, but a very low degree of order parallel to the Cu(111) surface. No differences in our results were detected for measurements at room temperature versus at ~ 190 K.

1. Introduction

The adsorption of alkali atoms on metal surfaces has for a long time been the subject of both experimental and theoretical studies [1]. The interest in these systems is due in large part to the expectation that the alkalis serve as good model systems for studying metal adsorption and the metallization of overlayers on surfaces. The study of the geometry of alkali metal adsorbates and alkali-induced changes in the substrate structure for alkalis adsorbed on metal surfaces has revealed surprising results in the past few years [2–9]. For one, it was previously assumed

that alkalis adsorb in high-coordination sites on low index, atomically flat metal surfaces due to their simple electronic structure. However, recent experimental evidence has shown that alkali adsorbates occupy top sites in several cases [2–9]. In addition, several recent studies of alkali adsorption have detected only small, if any, changes in alkali–substrate bond length as a function of increasing alkali coverage [10]. This suggests that early pictures of alkali adsorption and bonding which involve an ionic–metallic phase transition as a function of increasing coverage are not correct [1].

We previously performed a LEED study for the system Rb/Cu(111) at room temperature [11]. We found an ordered (2 × 2) phase for one monolayer of Rb on Cu(111), suggesting a single site of occupa-

* Corresponding author. Fax: +1 401 792 2380; E-mail: drhphy@uriacc.uri.edu.

tion. This observation made this system a good candidate for a more detailed investigation with the X-ray standing wave (XSW) technique [12–19]. In our previous publication [20] we reported detailed measurements of a structural study of Rb adsorption on Cu(111) for one layer of Rb ((2 × 2) LEED, $\theta = 0.25$) using the XSW technique in the back reflection geometry (BRXSW). We concluded that the Rb adsorption was in the top site on the Cu(111) surface, and we observed a high degree of Rb order perpendicular to the surface, but a lower degree of ordering parallel to the surface. In this paper, we extend our measurements to lower coverages and also report some measurements carried out below room temperature.

During dynamical Bragg diffraction from a single crystal, the incident and reflected X-ray plane waves interfere to set up a standing wave field parallel to and having the same spatial periodicity as the diffraction planes. By scanning (in angle or energy) through the finite range of the total reflectivity condition, the phase of this standing wave field shifts continuously relative to the atomic scattering planes. By measuring a yield characteristic of an adsorbate excited by the standing wave field, such as Auger, photoemission, or X-ray fluorescence, the atom's position relative to the diffraction planes can be determined. By combining results of standing wave measurements using sets of diffraction planes that are not parallel, the adsorbate's bonding site can also be determined by simple geometric triangulation. In addition, the degree of order of an adsorbate overlayer in different spatial directions can also be determined using the XSW technique.

2. Experimental

The experiments reported below were performed on beamline X25 at the National Synchrotron Light Source at Brookhaven National Laboratory. This beamline is a special high intensity line which extracts its radiation from a 27 pole hybrid wiggler which is installed in a straight section of the X-ray storage ring [21]. The beamline optics consist of a 1 : 1 double focusing mirror followed by a double crystal monochromator (Si(111) crystals were used in this experiment). In order to increase the flux at

the low X-ray energies required in this experiment (~ 3 keV), several graphite filters were removed from the beam path. To compensate for the increased heat load on the primary beryllium window, the wiggler field was cut in half to ~ 0.5 T. We estimate the net gain in flux at ~ 3 keV versus a bending magnet beamline (specifically comparing to our previous measurements on X19A and X24A) to be a factor of ~ 5. This allowed us to examine lower Rb coverages with greater sensitivity than was possible in our previous XSW runs.

The X25 beamline terminates in a Be window. The UHV chamber used in these experiments was attached to the beamline through two He-filled ion chambers and a thin Be window on the UHV chamber itself. The ion chambers were used to record the incident and back-reflected X-ray intensities. The UHV chamber was equipped with a single pass cylindrical mirror analyzer (CMA), an ion sputter gun, an alkali doser, and other standard UHV instrumentation. A base pressure in the low 10^{-10} Torr range was achieved.

The Cu(111) sample was cleaned by Ar^+ sputtering and annealing to 700 K for 5 min. The crystal was clamped onto a tantalum plate attached to a button heater which was used to raise the temperature of the sample. A chromel–alumel thermocouple clamped to the crystal was used for temperature measurements. Sample cleanliness was monitored by XPS. The Rb was evaporated from a commercial SAES Getter source equipped with a shutter and collimation. The background pressure rise in the chamber during evaporation was less than 1×10^{-10} Torr. The coverage was determined by correlating work function measurements and dose times with our previous LEED and work function measurements of this system [11] and by measuring the coverage dependence of the photoemission intensity of the $Rb 2p_{3/2}$ core level excited by the incident X-ray beam. In our LEED study, we observed a (2×2) overlayer structure for one layer of Rb on Cu(111), which corresponds to a coverage of $\theta = 0.25$, an Rb surface density of 1 Rb atom per 4 Cu(111) substrate atoms. This coverage assignment is consistent with previous LEED observations of (2×2) overlayers for both K/Cu(111) and Cs/Cu(111) [22]. At lower coverages of Rb/Cu(111), no new LEED structures besides a (1×1) pattern were observed. All Rb

dosing and all measurements, unless otherwise noted, were performed at room temperature.

The back reflection X-ray standing wave (BR-XSW) experiments were conducted by setting either the (111) or (11$\bar{1}$) planes of the Cu(111) crystal perpendicular to the incident monochromatized X-ray beam and monitoring the diffracted beam which is diffracted directly back from the crystal planes in a direction antiparallel to the incident beam. For the (111) reflection, the X-ray beam was incident normal to the sample surface. For the (11$\bar{1}$) reflection, the X-rays were incident at 70.53° to the surface normal, but the diffraction was still carried out in the symmetric, back reflection geometry.

In XSW measurements, the heights or intensities of one or more core level, Auger, or fluorescence peaks are recorded along with the background intensity as the photon energy (or in some cases, the incident angle) is scanned around the Bragg diffraction peak. The background levels are then subtracted from the peak heights and the result is plotted versus photon energy. In our investigation, we typically scanned the photon energy over a 6 eV range in steps of 0.1 eV. We recorded the electron yields for the Rb$2p_{3/2}$ peak, one or more Cu LMM Auger peaks, Cu core levels in some cases, and the background height for each peak taken at 10 eV above the peak for the Rb$2p_{3/2}$ case. (For the core level measurements, the analyzer kinetic energy was stepped along with the monochromator to stay on the peak.) Finally, we simultaneously recorded the X-ray reflectivity using He-filled ion chambers placed in the beam path.

3. Results

3.1. XSW analysis

In Fig. 1 are presented a series of electron energy distribution curves (EDC's) for the (2 × 2) Rb/Cu(111) overlayer obtained at different incident X-ray photon energies. These EDC's include electron emission from both the Cu LMM Auger region and the Rb$2p$ core levels. The curve labeled with a relative photon energy of "0.0 eV" corresponds to a spectrum recorded at an X-ray energy corresponding to the peak of the X-ray reflectivity rocking curve or
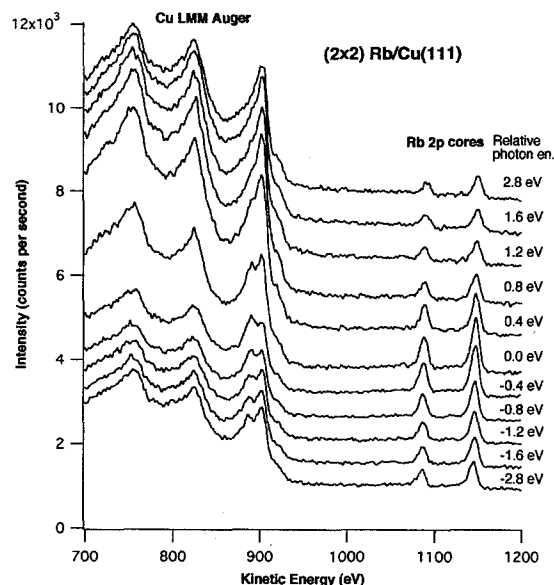
Fig. 1. Electron energy distribution spectra for one monolayer of Rb on Cu(111) as a function of photon energy relative to the rocking curve maximum (at 2974.5 eV). The Cu LMM Auger peaks and the Rb$2p$ core level photoemission peaks are indicated. The X-ray photon beam was incident normal to the crystal in the [111] direction. All the curves in this figure are on the same absolute scale, but the upper curves have been offset by varying amounts from the bottommost (−2.8 eV) curve for display purposes.

Bragg diffraction condition (2.9745 keV) for the back reflection geometry normal to the Cu(111) Bragg planes. The other curves in Fig. 1 were recorded at X-ray energies in 0.4 eV steps relative to this photon energy. If we concentrate on the Rb$2p$ region, it is clear that there is a significant variation in the intensity of the Rb peaks over this narrow photon energy range. A closer examination shows that the Rb cores have their greatest intensity at a photon energy between 0.0 and −0.4 eV (relative to the Bragg peak energy). This displacement from the Bragg peak is due to the X-ray standing wave field which is generated in and above the copper substrate; the exact photon energy dependence of the intensity of the Rb core levels gives very precise information on the position and ordering of the adsorbate overlayer. In contrast, for the Cu LMM Auger peaks the greatest intensity is clearly on the high photon energy side of the Bragg peak.

Now the peak height is subtracted from the corresponding background level and plotted versus photon
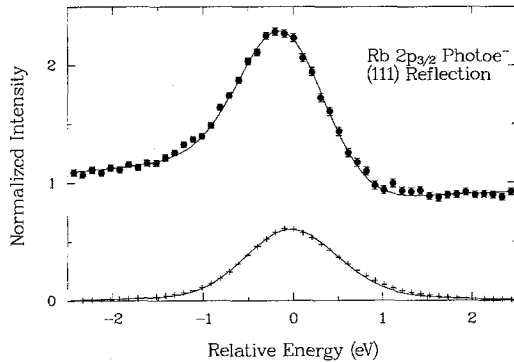
Fig. 2. Photon energy dependence of the $Rb\,2p_{3/2}$ core level photoelectron standing-wave yield for the (111) reflection plane (upper data set). The lower data set is the measured reflectivity, and the solid lines are fits using dynamical diffraction theory. For this data set, we obtained a coherent position and a coherent fraction of 0.39 ± 0.01 and 0.71 ± 0.02, respectively.

energy. Typical data sets for the $Rb\,2p_{3/2}$ core level and for one of the Cu LMM Auger peaks are presented in Figs. 2 and 3, respectively. In the Rb data, the photoelectron yield has its maximum close to a relative photon energy of -0.2 eV; on the other hand, the Cu LMM Auger yield maximum occurs at about $+0.5$ eV above the diffraction peak energy. These results are consistent with our qualitative observations of the Rb and Cu peak intensities in Fig. 1, as discussed above. For Rb, if the atoms were randomly distributed in the [111] direction, then all
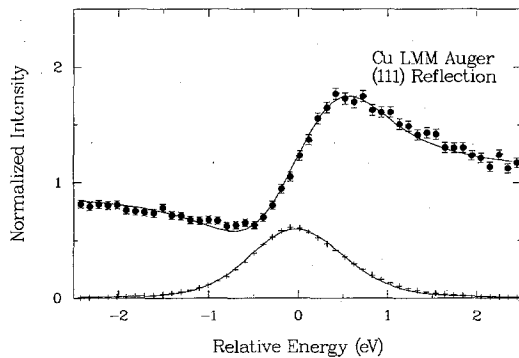
Fig. 3. Photon energy dependence of the 840 eV Cu LMM Auger electron standing-wave yield for the (111) reflection plane (upper data set). The lower data set is the measured reflectivity, and the solid lines are fits using dynamical diffraction theory. For this data set, we obtained a coherent position and a coherent fraction of -0.02 ± 0.01 and 0.93 ± 0.02, respectively.
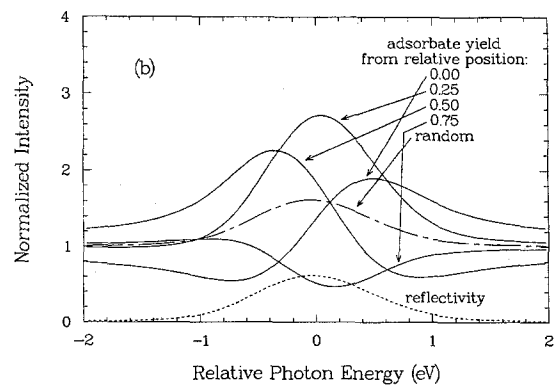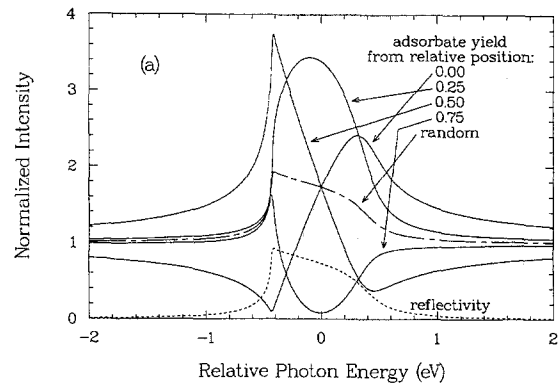
Fig. 4. Theoretical XSW results for various positions of an adsorbate on Cu(111) in units of the fraction of the Cu(111) d-spacing (2.08 Å). The theoretical rocking curves (labeled "reflectivity") are also plotted. The curves in (a) are ideal; in (b) they have been broadened by a convolution with the monochromator reflectivity profile and with a Gaussian function with FWHM of 0.8 eV (a 2σ of 0.7 eV).

peak intensities would simply track the X-ray reflectivity. Already from our data we can be confident that the Rb atoms are ordered in the [111] direction and, from a comparison of Figs. 2 and 3, are sitting rather "far" (on our 2 Å d-spacing scale) from bulk-like copper positions since the yield maxima are on opposite sides of the Bragg peak. Further analysis requires a comparison to simulations of XSW yields derived from dynamical diffraction theory.

In Fig. 4a we present a series of ideal theoretical XSW yield curves assuming different adsorbate positions. These curves have been broadened in Fig. 4b by convolution with the 2-bounce monochromator

profile (the square of the Darwin reflectivity from a single bounce) and with a Gaussian function to take account of the energy broadening arising from dispersion between the monochromator and sample, and of the finite mosaicity of the substrate.

For emission from atoms sitting on bulk lattice sites, the XSW yield looks like that labelled "0.00" in Fig. 4 (this is the coherent position in units of the Cu(111) d-spacing, 2.08 Å), since when the photon energy is set on the high side of the Bragg peak (at higher photon energy), the standing wave field has its maximum intensity (antinode) on the diffraction planes and its minimum intensity (node) midway between the diffraction planes. In contrast, when the photon energy is set on the low side of the Brag peak the positions of the antinode and node are reversed. Therefore, for atoms sitting exactly midway between bulk lattice sites, the standing wave yield looks like that labelled "0.50" in Fig. 4. For emission from atoms sitting elsewhere, the maxima and minima of the yield curves occur at different photon energies about the Bragg peak (e.g. the yield curves labelled "0.25" and "0.75"), corresponding to interstitial positions in units of the d-spacing.

Since in our experiment, the (bulk) copper atoms should be on the copper lattice sites, the XSW curve we measured for the Cu LMM Auger peak (Fig. 3) should resemble the simulation for a coherent position of 0.00; and the data are in good qualitative agreement with this simulation. Our Rb $2p_{3/2}$ results (Fig. 2) are closest to but a little bit off from the curve labeled "0.50" in Fig. 4b (somewhere between the "0.50" and the "0.25" curves). Therefore just by an inspection of our XSW data we can already estimate an Rb coherent position of ~ 0.4, which corresponds to a position for the Rb atoms of (~ 0.4) × (2.08 Å) ≈ 0.8 Å above a Cu(111) lattice plane.

To obtain more quantitative information regarding the geometry of the Rb overlayer, we must first extract several non-structural parameters from our data, the most important of which is an estimate of the instrumental broadening and mosaic spread of the crystal. This is done by convoluting with a Gaussian function the convolution of the ideal Darwin–Prins reflectivity curve of monochromator and sample as predicted from dynamical diffraction theory (the dot-dashed curve in Fig. 4a is such a

theoretical reflectivity curve) and matching this to our experimental reflectivity measurements (lower curves in Figs. 2 and 3). The X-ray reflectivity curve in the ideal case is broadened into a fairly symmetric, Gaussian-like curve (see the dot-dashed curve in Fig. 4b) through a combination of the effects of finite instrumental resolution and the mosaic spread of the Cu(111) crystal (which we previously measured to be ~ 0.25°). When we carried out this convolution procedure, the result of which is given by the lower solid curves in Figs. 2 and 3, we obtained a Gaussian broadening of 0.7 eV. We use this factor in subsequent analysis of the XSW data.

In the next step, this Gaussian broadening function (again after convolution with the monochromator reflectivity profile) is convoluted with ideal XSW curves (Fig. 4a) to generate a series of simulations for different positions of the adsorbate above the surface, as was presented in Fig. 4b. These simulations are then compared to the data until the best match is obtained using a χ^2 fitting procedure. From this procedure, the position of the adsorbate is derived. The results of such analysis for the copper and rubidium positions are given by the upper solid curves in Figs. 2 and 3. The geometric parameters obtained from this analysis are discussed below.

A more formal description of the adsorbate photo-electron-yield in the standing wave field is given by [16]:

$$Y(\mathscr{E})/Y_{0B}$$

$$= 1 + R(E) + 2\sqrt{R(E)}\,f\cos\left[\nu(\mathscr{E}) - 2\pi\phi\right].$$

Here the reflectivity is $R(E) = |E_H/E_0|^2$, where E_0 and E_H are the incident and diffracted beam electric field amplitudes, respectively; $\nu(\mathscr{E})$ is the energy-dependent phase of E_H relative to E_0; Y_{0B} is the emission yield away from the Bragg reflection; and ϕ and f are the so-called coherent position and coherent fraction. They represent, respectively, the weighted average position of the atoms relative to the diffraction planes and the spread of positions of the adsorbate atoms. The coherent position takes on a value between 0 and 1, with a value of 0 or 1 corresponding to a position on the planes (i.e. the curve labelled "0.00" in Fig. 4), and ±1/2 corresponding to a position midway between the planes (the curve labelled "0.50" in Fig. 4). The coherent

fraction comprises the product of a thermal Debye–Waller factor for the adsorbate, a factor determined by static disorder, and a geometric factor which includes the effect of multiple-site adsorption relative to the reflecting planes. A value of unity for the coherent fraction means that all the adsorbate atoms are located at the same (coherent) position relative to the diffraction planes, while a value of less than 1 for the coherent fraction means that more than one position is occupied or there is some type of disorder in the system. Therefore, in addition to the positions of the adatoms, the degree of ordering is also obtained from the XSW analysis. This is accomplished by requiring that the simulations match not only the peak positions, but also reproduce the relative heights of the XSW curves above the baseline (given by the yield at photon energies removed from the Bragg peak). For randomly positioned absorbers (dot-dashed curves in Fig. 4), corresponding to a coherent fraction of 0, the XSW simulations just trace the reflectivity curves with an offset given by the off-Bragg absorbate yield.

3.2. (2 × 2) Rb / Cu(111) results

3.2.1. The [111] reflection

The results of our analysis for the Rb/Cu(111) data presented in Figs. 2 and 3 are shown by the solid lines. For the Rb result, this particular data set yielded a coherent position of 0.39 ± 0.01 and a coherent fraction of 0.71 ± 0.02. This final position is close to our estimate from a visual comparison of the data and simulations as discussed above. The coherent fraction indicates a relatively high degree of ordering of the Rb atoms in the direction perpendicular to the surface. The fit to the Cu Auger yield (Fig. 3) produced a coherent position and coherent fraction of −0.02 ± 0.01 and 0.93 ± 0.02, respectively. As expected, since a measurement of the copper Auger electrons (mean free path ~ 10 Å) mainly probes the copper bulk lattice positions, the coherent position should be near 0 and the coherent fraction should be high (near 0.97, the Debye–Waller factor of Cu(111) at room temperature).

In the XSW investigation reported here, we carried out several measurements of the Rb positions for this coverage and reflection geometry. In all cases in the [111] geometry, we obtained coherent
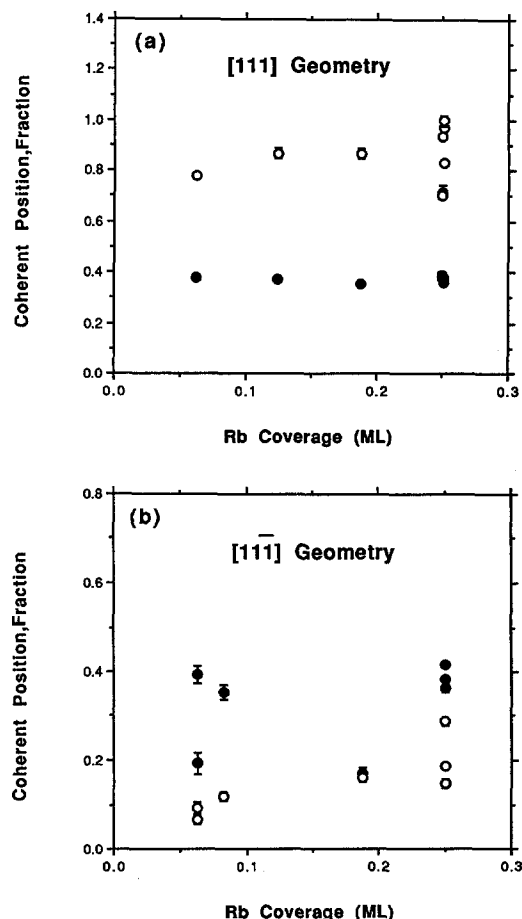
Fig. 5. Summary of the coherent positions and coherent fractions obtained from our XSW measurements of Rb/Cu(111) as a function of Rb coverage for both the [111] and [11$\bar{1}$] reflections. The [11$\bar{1}$] data includes results taken at both room temperature and at 190 K. Each set of points ((●) coherent position and (○) coherent fraction) represents a different surface preparation. The error bars shown in these figures were determined from the counting statistics for each individual set of data.

positions for the overlayer in the range of 0.35–0.39, and high coherent fractions between 0.7 and 1.0 (the results from several different preparations are presented in Fig. 5). In our previous publication [20], we reported a result of 0.47 for the coherent position (with also a high coherent fraction), which is not in agreement with our current results for the Rb position of the monolayer. At this time, we attribute this discrepancy to some difference in surface conditions or preparation in our previous runs. Previously [20],
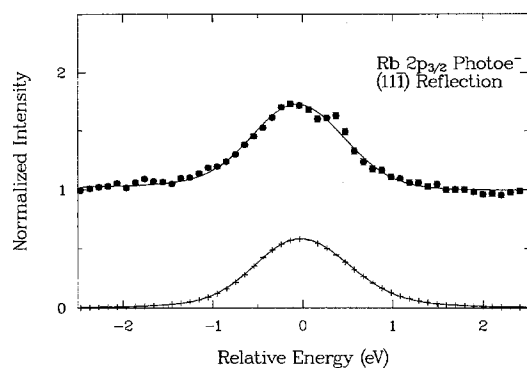
Fig. 6. Photon energy dependence of the $Rb 2p_{3/2}$ core level photoelectron standing-wave yield (upper curve) for the $(11\bar{1})$ reflection plane for one monolayer of $Rb/Cu(111)$, and the measured reflectivity (lower curve). The solid lines are fits using dynamical diffraction theory. For this data set, we obtained a coherent position and a coherent fraction of 0.36 ± 0.01 and 0.15 ± 0.01, respectively.

we had observed a time dependence in the measured coherent fractions in the $[11\bar{1}]$ geometry which indicated some instability in the overlayer, probably due to contamination. In contrast, in our current investigation, all of our results were very stable and reproducible.

3.2.2. The [11̄1̄] reflection

This result above only provides the Rb position and degree of order perpendicular to the Cu(111) surface. To obtain additional structural information, we performed XSW backscattering measurements in the $[11\bar{1}]$ direction. We positioned the Cu(111) crystal at an angle of $\sim 70.5°$ with respect to the incident X-ray beam (but still maintaining a back reflection geometry) so this measurement probes the position and order of the adsorbate normal to the $(11\bar{1})$ Bragg planes and mostly parallel to the (111) surface. In Fig. 6 we present the results of one particular set of measurements for the full Rb layer in this configuration. A comparison to the corresponding curve from the [111] geometry (Fig. 2) shows a significant difference. For our $[11\bar{1}]$ measurements, the peak in the XSW Rb photoelectron yield coincides with the peak of the reflectivity rocking curve; in addition, the relative height of the yield is much smaller than for the [111] case. This data set is in fact quite similar to the dot-dashed curve in Fig. 4b of a simulation of the

yield expected for randomly positioned adsorbates. We therefore expect that this measurement will yield a relatively low coherent fraction, which will indicate a loss of ordering of the Rb atoms in the $[11\bar{1}]$ direction.

When this particular data set was subjected to a more detailed XSW analysis, we obtained geometric parameters of 0.37 ± 0.01 for the $[11\bar{1}]$ coherent position, and 0.20 ± 0.01 for the $[11\bar{1}]$ coherent fraction. As anticipated in the discussion above, the coherent fraction and corresponding ordering is low in this direction, which is in qualitative agreement with our previous results [20].

3.3. Rb coverage dependence

We have now performed several measurements of the Rb adatom geometry for a series of submonolayer coverages. We find that for all of the coverages we have examined, from 0.25 to 1 layer, the corresponding [111] coherent fractions are always high (> 0.7) and the [111] coherent positions are quite constant (~ 0.37). Our BRXSW results for the coherent positions and coherent fractions for $Rb/Cu(111)$ in the [111] geometry as a function of coverage are summarized in Fig. 5a. It is clear from these results that the Rb overlayer is always well-ordered in the [111] direction for all coverages, and that no significant change in position is detected.

We repeated many of our coverage-dependent measurements using the $[11\bar{1}]$ reflection to obtain in-plane adatom structural information, with the results summarized in Fig. 5b. The significant result is that for all coverages we obtained coherent fractions of 0.1–0.3 or lower.

3.4. Low temperature measurements

Primarily with the goal of examining the degree of order of the Rb atoms in the $[11\bar{1}]$ direction, we also carried out some BRXSW measurements at lower temperature (~ 190 K). For these measurements, we still deposited the Rb at room temperature; then we cooled the sample with liquid nitrogen to the lowest temperature achievable in our current experimental arrangement, which turned out to be 190 K. We performed these measurements for several coverages, mostly in the $[11\bar{1}]$ geometry. We

observed no significant change in coherent position or coherent fraction at 190 K versus at room temperature.

4. Discussion

As summarized and plotted in Fig. 5, we detected an almost constant coherent position in the [111] direction for the Rb atoms as a function of coverage down to relatively low coverages. This indicates that there is little or no change in the perpendicular spacing of the Rb atoms above the copper substrate as a function of Rb coverage. In addition, we find from the high [111] coherent fractions, that the Rb overlayer maintains a high degree of ordering perpendicular to the surface throughout the coverage range investigated. These high coherent fractions suggest that the Rb atoms maintain the same bonding site at all coverages; however, the low coherent fractions we obtained in the [11$\bar{1}$] direction make it impossible for us to triangulate to the bonding site unambiguously.

Regarding the issue of bond length changes as a function of coverage, several recent investigations of alkali overlayers have detected little or no change in alkali–substrate bond length, or hard sphere radius, as a function of coverage [10]. This is certainly consistent with our present results. However, our XSW measurements are not directly sensitive to changes in the Cu(111) surface geometry. Therefore, though unlikely, we cannot rule out some combination of Rb site changes and substrate surface changes which result in a constant, coverage-independent coherent position in the [111] direction. We hope that a future investigation at a lower temperature will produce higher coherent fractions in the [11$\bar{1}$] direction, allowing us to triangulate to the Rb bonding site(s) at submonolayer coverages.

The loss of order parallel to the Cu(111) surface at all Rb coverages, as indicated by the very low coherent fractions we obtained for the [11$\bar{1}$] geometry, is quite significant particularly considering the consistently high coherent fractions we obtained for all coverages in the [111] direction. A similar loss of ordering in the parallel direction has also been reported by Kerkar et al. [5] in their XSW investigation of Rb/Al(111), by Adler et al. [8] in their SEXAFS investigation of K/Cu(111) and K/Ni(111), and by

Stampfl et al. [6] in a LEED study of K/Al(111). In all three cases the results were attributed to anisotropic vibrational amplitudes parallel to the substrate surface. It should be pointed out that in the latter two investigations, the measurements were carried out at significantly lower temperatures than was achievable in our present investigation: 70 K for K/Ni(111), Cu(111) [8] and 90 K for K/Al(111) [6].

There are several factors which could contribute to the low coherent fractions in our present XSW investigation of Rb/Cu(111). The most important of these are a large vibrational amplitude (Debye–Waller type effect), as proposed in the analogous studies mentioned above, or multiple site adsorption, either through averaging over more than one preferred site within the (11$\bar{1}$) diffraction plane or through static disorder, or both. Since the coherent fractions are always very high in the [111] direction, the existence of multiple bonding sites seems less likely, but cannot be excluded. On the other hand, if we assume that the low [11$\bar{1}$] coherent fractions are due solely to large vibrational amplitudes parallel to the surface, then we must require an RMS vibrational amplitude of 0.59 Å to account for a coherent fraction of 0.2, with some of our measurements yielding even *lower* coherent fractions than this. This should be compared to a value of 0.3 Å for the average lateral displacement of K/Al(111) at 150 K obtained by Stampfl et al. [6] in their LEED investigation, and a value of 0.18 Å for the vibrational amplitude of Rb/Al(111) at 190 K from the XSW study of Kerkar et al. [5]. Another possibility which could account for our results is that the Rb atoms are rather free to diffuse over the Cu(111) surface at all coverages. As long as the atoms maintain the same height above the surface, then the coherent fraction in the [111] direction would be high, as observed. Several authors have pointed out the flatness of the surface potential found in theoretical analyses of alkali/close-packed surface systems [4,6,23].

In summary, we have carried out a back reflection X-ray standing wave investigation of the system Rb/Cu(111) as a function of Rb coverage. We observed no change in the Rb–Cu perpendicular spacing as a function of coverage down to low, submonolayer coverages. We detected a high degree of ordering of the Rb atoms perpendicular to the

surface at all coverages, but a very low degree of order parallel to the Cu(111) surface. We found no differences in our results for measurements at room temperature versus at ~ 190 K.

Acknowledgements

References

[1] T. Aruga and Y. Murata, Prog. Surf. Sci. 31 (1989) 61; H.P. Bonzel, A.M. Bradshaw and G. Ertl, Eds., Physics and Chemistry of Alkali Metal Adsorption (Elsevier, Amsterdam, 1989), and references therein.

[2] S.Å. Lindgren, L. Wallden, J. Rundgren, P. Westrin and J. Neve, Phys. Rev. B 28 (1983) 6707.

[3] H. Over, H. Bludau, M. Skottke-Klein, G. Ertl, W. Moritz and C.T. Campbell, Phys. Rev. B 45 (1992) 8638.

[4] D. Fisher, S. Chandavarkar, I.R. Collins, R.D. Diehl, P. Kaukasoian and M. Lindroos, Phys. Rev. Lett. 68 (1992) 2786; P. Kaukasoian, M. Lindroos, R.D. Diehl, D. Fisher, S. Chandavarkar and I.R. Collins, J. Phys. C. 5 (1993) 2875.

[5] M. Kerkar, D. Fisher, D.P. Woodruff, Robert G. Jones, R.D. Diehl and B. Cowie, Phys. Rev. Lett. 68 (1992) 3204.

[6] C. Stampfl, M. Scheffler, H. Over, J. Burchhardt, M. Nielsen, D.L. Adams and W. Moritz, Phys. Rev. Lett. 69 (1992) 1532; Phys. Rev. B 49 (1994) 4959.

[7] Z. Huang, L.Q. Wang, A.E. Schach von Wittenau, Z. Hussain and D.A. Shirley, Phys. Rev. B 47 (1993) 13626.

[8] D.L. Adler, I.R. Collins, X. Liang, S.J. Murray, G.S. Leatherman, K.D. Tsuei, E.E. Chaban, S. Chandavarkar, R. McGrath, R.D. Diehl and P.H. Citrin, Phys. Rev. B 48 (1993) 17445.

[9] M.M. Nielsen, J. Burchhardt, D.L. Adams, E. Lundgren and J.N. Andersen, Phys. Rev. Lett. 72 (1994) 3370; J. Burchhardt, M.M. Nielsen, D.L. Adams, E. Lundgren and J.N. Andersen, Phys. Rev. B 50 (1994) 4718.

[10] Th. Hertel, H. Over, H. Bludau, M. Gierer and G. Ertl, Surf. Sci. 301 (1994) 1.

[11] C. Su, X. Shi and D. Heskett, unpublished results.

[12] D.P. Woodruff, D.L. Seymour, C.F. McConville, C.E. Riley, M.D. Crapper, N.P. Prince and R.G. Jones, Surf. Sci. 195 (1988) 237.

[13] B.W. Batterman, Phys. Rev. 133 A (1964) 759; Phys. Rev. Lett. 22 (1969) 703.

[14] P.L. Cowan, J.A. Golovchenko and M.F. Robbins, Phys. Rev. Lett. 44 (1980) 1680.

[15] J.A. Golovchenko, J.R. Patel, D.R. Kaplan, P.L. Cowan and M.J. Bedzyk, Phys. Rev. Lett. 49 (1982) 560.

[16] J. Zegenhagen, Surf. Sci. Rep. 18 (1993) 199.

[17] M.J. Bedzyk, D.H. Bilderback, G.M. Bommarito, M. Caffrey and J.S. Schildkraut, Science 241 (1988) 1788.

[18] L.E. Berman, B. Batterman and J.M. Blakely, Phys. Rev. B 38 (1988) 5397.

[19] H.D. Abruna, G.M. Bommarito and D. Acevedo, Science 250 (1990) 69.

[20] X. Shi, C. Su, D. Heskett, L.E. Berman, C.-C. Kao and M.J. Bedzyk, Phys. Rev. B 49 (1994) 14638.

[21] L.E. Berman, J.B. Hastings, T. Oversluizen and M. Woodle, Rev. Sci. Instrum. 63 (1992) 428.

[22] W.C. Fan and A. Ignatiev, J. Vac. Sci. Technol. A 6 (1988) 735; Phys. Rev. B 37 (1988) 5274; W.C. Fan, A. Ignatiev and B. Hu, Phys. Rev. B 39 (1989) 6816.

[23] J. Neugebauer and M. Scheffler, Phys. Rev. B 46 (1992) 16067.